ChemComm

COMMUNICATION

Cite this: *Chem. Commun.*, 2018, **54**, 539

Received 9th October 2017,
Accepted 13th December 2017

DOI: 10.1039/c7cc07812a

rsc.li/chemcomm

Water soluble two-photon fluorescent organic probes for long-term imaging of lysosomes in live cells and tumor spheroids†

Pratibha Kumari,[a] Sanjay K. Verma[b] and Shaikh M. Mobin*[abc]

The morphological alteration of lysosomes is a powerful indicator of various pathological disorders. In this regard, we have designed and synthesized a new water soluble fluorescent Schiff-base ligand (L-lyso) containing two hydroxyl groups. L-lyso exhibits excellent two-photon properties with tracking of lysosomes in live cells as well as in 3D tumor spheroids. Furthermore, it can label lysosomes for more than 3 days. Thus, L-lyso has an edge over the commercially available expensive LysoTracker probes and also over other reported probes in terms of its long-term imaging, water solubility and facile synthesis.

Lysosomes are acidic, membrane-bound organelles considered as ''stomachs'' of the cells, which degrade macromolecules delivered by endocytosis and intracellular materials with the help of multiple acid hydrolases.[1] Lysosomes play an important role in many physiological activities such as cell migration, cell signalling, cholesterol homeostasis, initiation of apoptosis and tissue remodelling.[2] Lysosomal dysfunction causes various diseases including lysosomal storage diseases such as Tay-Sachs,[3] progression of cancer,[4] neurodegenerative diseases such as Parkinson's disease, Gaucher disease and others.[3–5] Thus, the ability to visualize lysosomal morphology is essential in order to understand the biological functions of lysosomes. LysoTracker probes such as Neutral Red (NR), DND-189, and DND-99 are expensive fluorescent dyes that have the tendency to specifically label lysosomes. However, these dyes have some limitations: (i) prolonged accumulation of LysoTracker probes in the intracellular environment increases the cellular pH, causing fluorescent dye quenching as well as physiological and morphological changes in the lysosomes and (ii) the low photostability limits their use for long term tracking of lysosomes to observe dynamic changes in lysosomal morphology in a stipulated time.[6]

So far reports on long term imaging of lysosomes have been based on some metal-complexes,[7] BODIPY moieties,[8] complex organic or dextran-conjugated fluorophores,[9] (Chart S1, ESI†) and inorganic nanocomposites[10] but all these involve a tedious multistep synthetic process. Also, these emerging lyso-probes and nanoparticles may suffer from toxic impacts.[11] For example, the SiO_2 particles are well known to cause damage to the lysosomal membranes.[12] Moreover, the dextran based fluorescence lysotracker cannot be used for long term imaging due to the inherent toxicity of dextran towards lysosomal functions.[13] Among these fluorophores, some of them have short wavelength excitation leading to cellular auto-fluorescence resulting in photodamage and photobleaching.

To overcome the above limitations, we need small water soluble organic probes having two-photon (TP) fluorescence properties. Owing to the low background interference, minimal photodamage of cells or tissues, penetration depth (>500 μm) and near-infrared light (700–1100 nm) excitation wavelengths,[14] two-photon microscopy (TPM) is an essential tool for bioimaging within intact tissue and live cells.

Herein, we have designed and synthesized a one-step Schiff-base organic probe **L-lyso** in a facile manner by condensation of 4-(diethylamino)-2-hydroxybenzaldehyde and 3-amino-2-hydroxynaphthalene (Scheme 1). The **L-lyso** was characterized by standard spectroscopic methods *viz* FTIR, ^{1}H & ^{13}C NMR spectroscopy, and LC-MS and further authenticated by a single crystal X-ray diffraction study (Fig. S1–S4, ESI†).

The single crystal of **L-lyso** was grown in a methanol/chloroform solution by slow evaporation at 25 °C and crystallized in

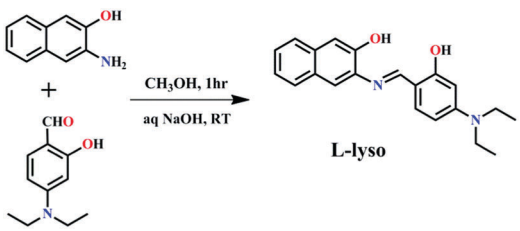

Scheme 1 Schematic representation of the synthesis of **L-lyso**.

[a] *Centre for Biosciences and Bio-Medical Engineering, Indore, India*
[b] *Discipline of Chemistry, Indore, India*
[c] *Metallurgical Engineering and Materials Science, Indian Institute of Technology Indore, Simrol Indore 453552, India. E-mail: xray@iiti.ac.in*

† Electronic supplementary information (ESI) available. CCDC 1570338. For ESI and crystallographic data in CIF or other electronic format see DOI: 10.1039/c7cc07812a

an orthorhombic crystal system with a noncentrosymmetry $Pna2_1$ space group (Tables S1, S2, ESI† and Fig. S5(a), ESI†). **L-lyso** is non-planar due to the presence of naphthyl and phenyl rings in two different planes attached from an imine (>C═N–) unit, with a torsion angle of 25.86°. The packing features of **L-lyso** reveal the presence of intra and inter molecular H-bonding interactions[15] (Fig. S5(b), ESI†). The intramolecular H-bonding interaction O(2)–H(1)···N(1), with a bond length of 1.924 Å, was observed between the hydroxyl group of the phenolic moiety and a nitrogen atom of the imine group (>C═N–). In the intramolecular H-bonding O(2)–H(1)···N(1) interactions, O(2)–H(1) is the donor and N(1) is the acceptor. While the intermolecular H-bonding interaction occurs between the phenolic moiety of one molecule and the naphthyl ring of the neighbouring unit, O(1)–H(1)···O(2), 1.764 Å, where O(1)–H(1) is the donor and O(2) is the acceptor, it leads to the formation of a 2D-network (Fig. S5(b), ESI†). Moreover, the π–π interaction,[16] 4.060 Å, between the phenyl and naphthyl rings, facilitates the charge transfer from the electron rich phenyl to the electron deficient naphthyl ring (Fig. S5(b) and S6, ESI†).

Furthermore, **L-lyso** is found to be an excellent candidate for two-photon (TP) excitation that has the ability to label lysosome in live cells as well as in tumor spheroids. TP fluorescent probes for the imaging of lysosomes are rare.[17] Moreover, most of them emit two-photon excited fluorescence near 500 nm, which is very close to the emission spectrum of the existing TP probes for other targets.[18] Therefore, TP **L-lyso** was designed, and it emits fluorescence in the short wavelength range (λ_{em} = 415–470 nm).

The lysosome pH is between 4.5 and 5.5.[7b] Therefore, the photophysical properties of **L-lyso** were studied in a disodium hydrogen phosphate/citric acid buffer at pH 5.5. The absorption bands of **L-lyso** were observed at 235, 349, and 429 nm which were attributed to the spin-allowed ligand-centred (LC) $\pi \rightarrow \pi^*$ and 452 nm for $n \rightarrow \pi^*$ transitions. The emission spectrum of **L-lyso** at an excitation wavelength of 280 nm exhibited the highest intensity at 383 nm (Fig. S7a, ESI†). The fluorescence intensity of **L-lyso** was quite stable up to pH 8.3 (Fig. S7b, ESI†). The fluorescence intensity of **L-lyso** quenching, slightly at high pH, may be due to the formation of the electron donor phenoxide ion, through photoinduced electron transfer (PET) under basic conditions. Moreover, the highly elevated Stokes shift of 148 nm for **L-lyso** has added advantages over the commercially available LysoTrackers such as LysoTracker Green DND-26 (LTG) with a Stokes shift = 7 nm and LysoTracker Red DND-99 (LTR) with a Stokes shift = 13 nm.[19] Thus, the higher Stokes shift in **L-lyso** will restrict the cross-talk between the absorption and emission spectra and will allow distinguished peak separation with a high signal to noise ratio in cellular imaging. The two-photon emission intensities were compared at varying excitation wavelengths in the 700–830 nm range and were found to be maximum at λ_{ex} = 790 nm (Fig. S8, ESI†). The log–log linear relationship between the emission intensity and the incident power of **L-lyso** was measured at 790 nm using a femtosecond laser pulse and the resulting slope of 2.22 confirms the two-photon process (Fig. S9, ESI†). The retention of **L-lyso** inside the lysosomes may be probably explained by the low pK_a values of 3.27 for the amine and 3.55 for the imine present in **L-lyso**. The amine and imine groups present in **L-lyso** prefer the most acidic lysosomes compared to other subcellular organelles and are protonated inside the lysosomes which increases the hydrophilicity. Thus, the protonated amine and imine groups of **L-lyso** restrict its movement in the acidic lysosomes.

High cellular viability is necessary for long term imaging of lysosomes. The MTT assay result demonstrates that the **L-lyso** probe is highly biocompatible for cellular and physiological studies within the concentration range 10–80 μM (Fig. S10, ESI†) for 24 h incubation and further increasing the incubation time to up to 34 h still shows a high IC_{50} value of 600 μM (±2.783) (Fig. S11, ESI†).

Flow cytometry was used to acquire high quality fluorescence signals with high spatial resolution from significant populations of cells in flow.[7c,20] Hence, concentration dependent analysis was done by both flow cytometry and by confocal microscopic imaging. The fluorescence emitted by the cells (60 μM **L-lyso**) was more intense; hence, both the scatter plot and the histogram shifted more toward right (Fig. S12a and b, ESI†). Furthermore, cells treated with 0 μM (control), 30 μM and 60 μM **L-lyso** exhibit mean fluorescence intensities of 75, 953 and 1804, respectively. This indicates that **L-lyso** can uniformly label lysosomes over a large population of cells, which was detected in live suspension cells by flow cytometry and live adhered cells by microscopy (Fig. S12c, ESI†).

In order to investigate the binding of **L-lyso** to lysosomes, we examined the co-staining of MCF-7 cells with two organelle trackers LysoTracker Red DND-99 (LTR) for lysosomes and MitoTracker Red CMXRos for mitochondria separately (Fig. S13, ESI†). The pink staining in the overlay images was generated by superimposition of blue **L-lyso** and red organelle trackers, which shows that **L-lyso** have immense correlation with LysoTracker Red (Fig. S13a, ESI†) and is compatible for counter staining with MitoTracker Red (Fig. S13b, ESI†).

Furthermore, the universal lysosomal selective staining ability of **L-lyso** was evaluated in four different cell lines *i.e.*, HeLa (Cervical cancer), MCF-7 (breast cancer), A375 (skin melanoma) and DU145 (prostate cancer) cells (Fig. S14, ESI†). An excellent lysosome labeling pattern was achieved in all examined live cells. Moreover, the co-localization effect of **L-lyso** and LTR was evaluated by Pearson's co-localisation coefficient (R_r) (Fig. S15, ESI†). The overlapping fluorescence signals showed high Pearson's coefficients of 0.84, 0.83, 0.85 and 0.87 for HeLa, MCF-7, A375 and DU145 cells respectively, which were found to be the best among the reported lysosome probes.[21] Furthermore, Manders' coefficients were calculated indicating very good colocalization of the blue (**L-lyso**) and red (LTR) channels with each other on a per-pixel level (Table S3, ESI†).

Confocal microscopy was further used to explore the probable mechanistic pathways of cellular uptake of ligand **L-lyso**. HeLa cells were treated with **L-lyso** in two confocal dishes; one dish was incubated at 37 °C and the other at 4 °C to identify whether the uptake by the cells was *via* an energy-dependent (endocytosis) or an energy-independent transport pathway. The uptake of **L-lyso** by the cells at 4 °C as well as 37 °C suggested that it was taken up *via* an energy-independent pathway (Fig. S16, ESI†).

The photostability of the lysosome tracking probe is an essential parameter for long term imaging during physiological and morphological alterations.[6c] To examine the photostability of **L-lyso**, photo-bleaching experiments for both **L-lyso** and LysoTracker Red DND-99 in HeLa cells were performed and the results were compared. After 1800 scans the fluorescence intensity of LysoTracker Red was reduced to 2%, however the one-photon and two photon fluorescence intensity of **L-lyso** was 36% and 60% respectively (Fig. S17 and Movies S1–S3, ESI†). These results showed that **L-lyso** exhibits better photostability compared to commercial LysoTracker Red and is suitable for long term lysosomal bioimaging.

Two photon imaging is superior to one photon microscopy imaging in terms of low phototoxicity, low background signal, high photostability and more imaging depth (>500 μm).[22] Thus, we performed both one and two-photon co-localization imaging of **L-lyso** with LysoTracker Red which demonstrated a strong overlap in both cases (Fig. 1) and no autofluorescence from the cells and tumor spheroids was observed in the absence of **L-lyso** (Fig. S18–S20, ESI†).

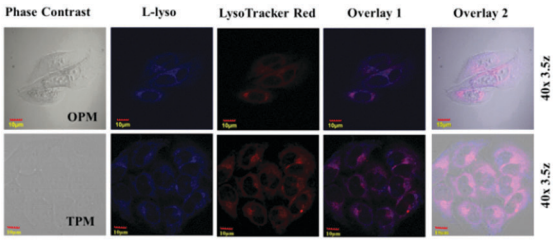

Fig. 1 One-photon microscopy (OPM) and two-photon microscopy (TPM) images of live HeLa cells. **L-lyso** co-stained with **L-lyso** (60 μM, 10 min) and LysoTracker Red DND-99 (80 nM, 10 min). **L-lyso**: λ_{ex} = 405 nm (OPM) or 790 nm (TPM). LysoTracker Red DND-99, λ_{ex} = 559 nm (OPM). Scale bar: 10 μm.

Lysosomes are involved in cell apoptosis and cell death which leads to lysosomal membrane permeabilization.[6a] Therefore, to focus on the tracking of lysosomes during apoptosis, we performed further studies. Carbonyl cyanide *m*-chloro-phenylhydrazone (CCCP) leads to the dysfunction of ATP synthase by reducing the mitochondrial membrane potential, resulting in inadequate ATP supply to the cells.[23] CCCP, an uncoupler of oxidative phosphorylation, was used to monitor the apoptosis. MitoTracker Red targets mitochondria by utilizing its membrane potential.[24] After addition of 20 μM CCCP, the red color stain of MitoTracker Red disappeared after 10 min (Fig. 2).

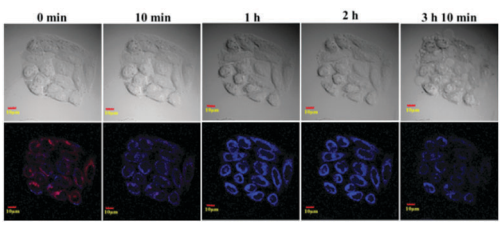

Fig. 2 Tracking lysosomes during apoptosis. Live HeLa cells stained with **L-lyso** (60 μM, 10 min) and MitoTracker Red CMXRos (80 nm, 10 min) and then with CCCP (20 μM) (here only the merged images are depicted for clarity).

This implies that the mitochondrial membrane potential starts abolishing and apoptosis is initiated. After 2 h, the cell morphology changes and apoptotic bodies begins to appear and after 3 h and 10 min, various apoptotic bodies were found. Simultaneously, the pH increases as a result of lysosomal membrane permeabilization, which causes a slight decrease in the intensity of blue fluorescence in most of the cells, further validating the pH based quenching of **L-lyso**, indicating lysosomal physiological conditions.

In order to simulate an *in vivo* environment, 3D tumor spheroids, which consist of cells in different phases *i.e.* proliferating, hypoxic, apoptotic and necrotic cells, were used. In 3D multicellular tumor spheroids, the cell–cell interactions as well as cell–extracellular matrix interactions prominently simulate the natural pattern of the body environment.[25]

The imaging of tumor spheroid depth layers through microscopy study still has many technical challenges.[26] Two spheroids of different sizes were labelled by **L-lyso** and the fluorescence images were taken after every 2 μm section cutting along the *Z*-axis. The TP fluorescence images of spheroid showed deeper and uniform tissue penetration in the deeper cell layer as compared to one-photon fluorescence microscopy, where the fluorescence intensity was observed up to ~46 μm (Fig. 3 and Fig. S21, S22, Movies S4–S6, ESI†). However, **L-lyso** does not remain intact during the formation of secondary spheroid (Fig. S23, ESI†). The results concluded that the two-photon excitation light has a deeper penetrating power. Thus **L-lyso** may be further utilized in the imaging of lysosomes in tissue.

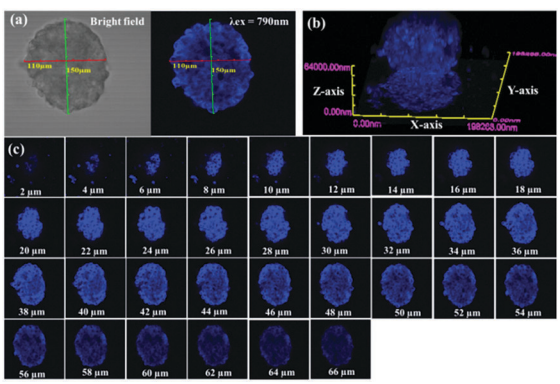

Fig. 3 (a) Two-photon fluorescence images of a 3D intact tumor spheroid 1 after incubation of **L-lyso** (60 μM) for 1 h. (b) The two-photon Z-stack 3D images of an intact spheroid. (c) The two-photon Z-stack images were captured after every 2 μm section from the top to bottom of the tumor spheroid. The images were captured under a 40× objective λ_{ex} = 790 nm; λ_{em} = 415–470 nm.

Lysosome tracking probes should possess the ability to stay in the lysosomes for a long period of time.[10a] Imaging of **L-lyso** was compared with LysoTracker Red (Fig. 4). After 2nd passage (48 h), the fluorescence signal of LysoTracker Red diminished completely, whereas the **L-lyso** fluorescence signal was still clearly visible even after 72 h. This justified that **L-lyso** could track lysosomes in live cells for at least 3 days (Fig. 4 and Fig. S24, ESI†). This confirmed the stable imaging of most of the physiological activities of the lysosomes in living cells.

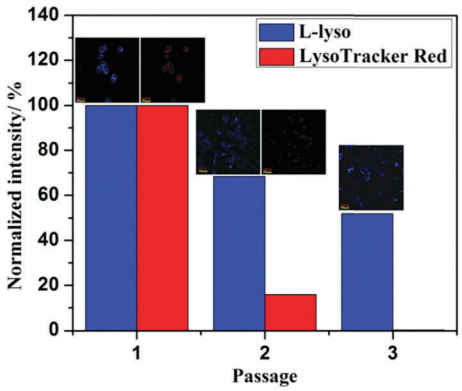

Fig. 4 Normalized fluorescence intensities and images of live HeLa cells, which were stained with 60 μM of **L-lyso** and 60 μM of LysoTracker Red at different passages. Scale bar: 30 μm.

In short, we have designed and synthesized a water soluble and non-cytotoxic organic probe, **L-lyso**, in a facile manner with high yield. Furthermore, **L-lyso** was confirmed to be an effective two-photon fluorescent probe for long-term tracking of lysosomes. The excellent two-photon properties of **L-lyso** were further explored using *in vivo* replica by employing in 3D multicellular tumor spheroids. **L-lyso** also enabled tracking of the lysosomes during cell apoptosis, and a mechanistic pathway for cell uptake has also been discussed. More importantly, **L-lyso** has a large Stokes shift (148 nm) and higher photostability compared to the commercially available Lyso-Tracker Red DND-99. These results of **L-lyso** may inspire the replacement of existing expensive and less stable lysosome specific dyes. The employment of **L-lyso** as a tracker can become a great contribution to the medical community and scientific community including industries.

The authors are grateful to the Sophisticated Instrumentation Centre (SIC), IIT Indore for providing characterization facilities. PK is thankful to MHRD, New Delhi for fellowship, SKV is grateful to SERB for providing National Postdoctoral Fellowship and SMM is thankful to SERB-DST (Project No, EMR/2016/001113), New Delhi, Govt. of India and IIT Indore for financial support.

Conflicts of interest

There are no conflicts to declare.

Notes and references

1 S. Aizawa, V. R. Contu, Y. Fujiwara, K. Hase, H. Kikuchi, C. Kabuta, K. Wada and T. Kabuta, *Autophagy*, 2017, **13**, 218.
2 (*a*) N. Raben and R. Puertollano, *Annu. Rev. Cell Dev. Biol.*, 2016, **32**, 255; (*b*) F. M. Platt, *Nature*, 2014, **510**, 68.
3 D. Dersh, Y. Iwamoto and Y. Argon, *Mol. Biol. Cell*, 2016, **27**, 3813.
4 P. Saftig and K. Sandhoff, *Nature*, 2013, **502**, 312.
5 T. Moors, S. Paciotti, D. Chiasserini, P. Calabresi, L. Parnetti, T. Beccari and W. D. van de Berg, *Mov. Disord.*, 2016, **31**, 791.
6 (*a*) A. Pierzynska-Mach, P. A. Janowski and J. W. Dobrucki, *Cytometry, Part A*, 2014, **85**, 729; (*b*) D. G. Smith, B. K. McMahon, R. Pal and D. Parker, *Chem. Commun.*, 2012, **48**, 8520; (*c*) X. Wang, D. M. Nguyen, C. O. Yanez, L. Rodriguez, H. Y. Ahn, M. V. Bondar and K. D. Belfield, *J. Am. Chem. Soc.*, 2010, **132**, 12237.
7 (*a*) L. He, Y. Li, C.-P. Tan, R.-R. Ye, M.-H. Chen, J.-J. Cao, L.-N. Ji and Z.-W. Mao, *Chem. Sci.*, 2015, **6**, 5409; (*b*) L. He, C. P. Tan, R. R. Ye, Y. Z. Zhao, Y. H. Liu, Q. Zhao, L. N. Ji and Z. W. Mao, *Angew. Chem., Int. Ed.*, 2014, **53**, 12137; (*c*) D. Y. Zhang, Y. Zheng, C. P. Tan, J. H. Sun, W. Zhang, L. N. Ji and Z. W. Mao, *ACS Appl. Mater. Interfaces*, 2017, **9**, 6761.
8 (*a*) J. Zhang, M. Yang, W. Mazi, K. Adhikari, M. Fang, F. Xie, L. Valenzano, A. Tiwari, F. T. Luo and H. Liu, *ACS Sens.*, 2016, **1**, 158; (*b*) H. Wang, Y. Wu, Y. Shi, P. Tao, X. Fan, X. Su and G. C. Kuang, *Chemistry*, 2015, **21**, 3219.
9 (*a*) C. Ji, Y. Zheng, J. Li, J. Shen, W. Yang and M. Yin, *J. Mater. Chem. B*, 2015, **3**, 7494; (*b*) X. Chen, Y. Bi, T. Wang, P. Li, X. Yan, S. Hou, C. E. Bammert, J. Ju, K. M. Gibson, W. J. Pavan and L. Bi, *Sci. Rep.*, 2015, **5**, 9004; (*c*) N. B. Yapici, Y. Bi, P. Li, X. Chen, X. Yan, S. R. Mandalapu, M. Faucett, S. Jockusch, J. Ju, K. M. Gibson, W. J. Pavan and L. Bi, *Sci. Rep.*, 2015, **5**, 8576; (*d*) T. Liu, Z. Xu, D. R. Spring and J. Cui, *Org. Lett.*, 2013, **15**, 2310; (*e*) Q. Wan, S. Chen, W. Shi, L. Li and H. Ma, *Angew. Chem., Int. Ed.*, 2014, **53**, 10916.
10 (*a*) H. Shi, X. He, Y. Yuan, K. Wang and D. Liu, *Anal. Chem.*, 2010, **82**, 2213; (*b*) Y. P. Ho and K. W. Leong, *Nanoscale*, 2010, **2**, 60.
11 Z. Li, Y. Song, Y. Yang, L. Yang, X. Huang, J. Han and S. Han, *Chem. Sci.*, 2012, **3**, 2941.
12 L. R. Farcal, C. Uboldi, D. Mehn, G. Giudetti, P. Nativo, J. Ponti, D. Gilliland, F. Rossi and A. Bal-Price, *Nanotoxicology*, 2013, **7**, 1095.
13 N. Ohno, T. Hashimoto, Y. Adachi and T. Yadomae, *Immunol. Lett.*, 1996, **52**, 1.
14 L. Zhu, W. Lv, S. Liu, H. Yan, Q. Zhao and W. Huang, *Chem. Commun.*, 2013, **49**, 10638.
15 A. K. Saini, K. Natarajan and S. M. Mobin, *Chem. Commun.*, 2017, **53**, 9870.
16 Y. C. Chang, Y. D. Chen, C. H. Chen, Y. S. Wen, J. T. Lin, H. Y. Chen, M. Y. Kuo and I. Chao, *J. Org. Chem.*, 2008, **73**, 4608.
17 S. Yao, H. Y. Ahn, X. Wang, J. Fu, E. W. Van Stryland, D. J. Hagan and K. D. Belfield, *J. Org. Chem.*, 2010, **75**, 3965.
18 (*a*) J. H. Son, C. S. Lim, J. H. Han, I. A. Danish, H. M. Kim and B. R. Cho, *J. Org. Chem.*, 2011, **76**, 8113; (*b*) S. Sumalekshmy and C. J. Fahrni, *Chem. Mater.*, 2011, **23**, 483.
19 LysoTracker and LysoSensor probes. Invitrogen. https://tools.thermofisher.com/content/sfs/manuals/mp07525.pdf.
20 W. L. Godfrey, D. M. Hill, J. A. Kilgore, G. M. Buller, J. A. Bradford, D. R. Gray, I. Clements, K. Oakleaf, J. J. Salisbury, M. J. Ignatius and M. S. Janes, *Microsc. Microanal.*, 2005, **11**, 246.
21 (*a*) B. Dong, X. Song, C. Wang, X. Kong, Y. Tang and W. Lin, *Anal. Chem.*, 2016, **88**, 4085; (*b*) F. Fan, S. Nie, D. Yang, M. Luo, H. Shi and Y. H. Zhang, *Bioconjugate Chem.*, 2012, **23**, 1309.
22 Q. Xu, C. H. Heo, G. Kim, H. W. Lee, H. M. Kim and J. Yoon, *Angew. Chem., Int. Ed.*, 2015, **54**, 4890.
23 J. S. Park, D. H. Kang and S. H. Bae, *Biochem. Biophys. Res. Commun.*, 2015, **464**, 1139.
24 Y. Chen, L. Qiao, L. Ji and H. Chao, *Biomaterials*, 2014, **35**, 2.
25 B. Patra, C. C. Peng, W. H. Liao, C. H. Lee and Y. C. Tung, *Sci. Rep.*, 2016, **6**, 21061.
26 P. Zhang, H. Huang, Y. Chen, J. Wang, L. Ji and H. Chao, *Biomaterials*, 2015, **53**, 522.

